Anisotropic Expansion of a Thermal Dipolar Bose Gas

Y. Tang,[1,2] A. G. Sykes,[3] N. Q. Burdick,[2,4] J. M. DiSciacca,[2,4] D. S. Petrov,[3] and B. L. Lev[1,2,4]
[1]*Department of Physics, Stanford University, Stanford, California 94305, USA*
[2]*E. L. Ginzton Laboratory, Stanford University, Stanford, California 94305, USA*
[3]*LPTMS, CNRS, University Paris Sud, Université Paris-Saclay, 91405 Orsay, France*
[4]*Department of Applied Physics, Stanford University, Stanford, California 94305, USA*
(Received 28 June 2016; revised manuscript received 29 August 2016; published 4 October 2016)

We report on the anisotropic expansion of ultracold bosonic dysprosium gases at temperatures above quantum degeneracy and develop a quantitative theory to describe this behavior. The theory expresses the postexpansion aspect ratio in terms of temperature and microscopic collisional properties by incorporating Hartree-Fock mean-field interactions, hydrodynamic effects, and Bose-enhancement factors. Our results extend the utility of expansion imaging by providing accurate thermometry for dipolar thermal Bose gases. Furthermore, we present a simple method to determine scattering lengths in dipolar gases, including near a Feshbach resonance, through observation of thermal gas expansion.

DOI: 10.1103/PhysRevLett.117.155301

Expansion imaging of a gas of atoms or molecules after it has been released from a trap provides a simple and highly valuable experimental tool for probing ultracold gases. For example, the technique is routinely used for thermometry by measuring the rate of gas expansion as it falls. The well-established procedure relies on the isotropic expansion of a thermal gas in which the interactions are negligible. Crucially, deviations from this isotropic behavior can provide a signature of the underlying interactions (and other complex phenomena) within the gas. Two notable examples of such deviation, caused by interacting systems confined in anisotropic traps, involve an aspect ratio (AR) inversion in nondipolar Bose-Einstein condensates (BEC) due to mean-field (MF) pressure forces arising from contact interactions [1,2] and in thermal Bose [3] and degenerate Fermi gases [4] in the collisional-hydrodynamic regime. Both effects alter the time-of-flight (TOF) dynamics and require a theoretical analysis to be understood [5]. The case of dipolar gases is more complicated since the anisotropy of the interaction also contributes to the TOF AR [6–8]. No theory exists for thermal dipolar Bose gas expansion even though such a theory is crucial for accurate thermometry.

In this Letter, we report on the anisotropic expansion of *thermal* bosonic ^{162}Dy and ^{164}Dy gases [9] and infer the temperature and scattering length from the TOF anisotropy. We find that the dominant physical mechanism responsible for the anisotropy comes from interatomic collisions which partially rethermalize the gas during the TOF. Non-negligible contributions arise also from Hartree-Fock mean-field interactions and Bose-enhancement factors. In particular, the resulting theory allows us to characterize the background scattering length and width of the 5.1-G Feshbach resonance in ^{162}Dy [10].

Our results pave a way toward investigations of ultracold gases in nontrivial regimes of classical fluid dynamics [11] where atomic collisions give rise to viscosity and turbulence [12]. Anisotropic dipolar interactions lead to a magnetoviscosity which has been studied in the context of classical ferrofluids in archetypal situations involving capillary flow [13]. While quantum ferrofluidity below condensation temperature T_c has been explored in Cr BECs [6], magnetoviscosity of dipolar Bose systems in the intermediate ultracold regime above T_c has yet to be explored. Such a regime is particularly relevant within the context of future progress toward connecting classical [12] and quantum [14] regimes of turbulence. It is therefore of fundamental interest that, in contrast to alkali atoms and Cr, this regime is accessible in these ultracold dysprosium gases with unsurpassed magnetic moment $\mu = 10\mu_B$ (Bohr magnetons).

Strongly dipolar lanthanide gases such as Dy and Er have additional complications associated with extremely dense spectra of Feshbach resonances revealed by atom-loss spectroscopy [10,15–17]. Such measurements provide the location, B_0, of individual resonances and have stimulated statistical studies on their distribution [16,18]. However, atom-loss spectroscopy alone cannot measure the resonance width ΔB [19], the remaining parameter that is required for quantitative control over the scattering length. To obtain ΔB, scattering lengths near a resonance must be measured. We demonstrate a particularly simple way of doing so by using fits of the thermal-gas AR expansion to our theory; a related technique was demonstrated for dipolar BECs [20].

We prepare ultracold gases of ^{162}Dy and ^{164}Dy following procedures described in Ref. [21]. In short, we perform laser cooling in two magneto-optical-trap stages, followed by forced evaporative cooling in a crossed optical dipole trap (ODT) formed by two 1064-nm lasers. During the evaporation, the magnetic field is along the z axis (along

gravity) and at a Feshbach resonance-free value of $B = 1.580(5)$ G [22]. To measure the AR in TOF of the gas, we suddenly turn off the trap and image the gas along the y axis after 16 ms using absorption imaging. We then fit the atomic density to a 2D-Gaussian function to extract the gas size σ_x and σ_z along $\hat{x}$ and $\hat{z}$ [23]. The gas AR is defined as σ_z/σ_x.

The dipolar thermal Bose gas used in our experiment consists of $N = 1.4(1) \times 10^5$ atoms for ^{162}Dy and $1.2(1) \times 10^5$ for ^{164}Dy. The atoms are prepared in the $|J = 8, m_J = -8\rangle$ ground state. To study the temperature dependence of the AR, we prepare the same number of atoms in the same trap but at different temperatures: First the gas is evaporated close to degeneracy, then the trap depth is increased, and finally we parametrically heat the gas to the desired temperature by modulating the ODT power. Before releasing the gas for TOF imaging, we let it thermalize in the trap for 1 s, which is much longer than the few-ms thermalization time scale [24]. The final trap frequencies are $[\omega_x, \omega_y, \omega_z] = 2\pi \times [107(1), 49(5), 266(1)]$ Hz for both isotopes. We note that this oblate trap geometry, where the confinement is the strongest along the magnetic field orientation $\hat{z}$, is necessary to avoid dipolar mechanical instabilities when evaporating towards T_c [25].

The measured gas AR at different temperatures are shown in Fig. 1. The errors include both statistical and systematic uncertainty and are dominated by systematic error, which we estimate to be 1% [26]. We measure an anisotropy as large as 9% for ^{162}Dy at 200 nK—just below T_c—with the field along $\hat{z}$. The anisotropy decreases with higher temperature, or when the magnetic field points along the imaging axis $\hat{y}$, such that the dipolar interaction is symmetric in the imaged x-z plane. The same trend is evident for ^{164}Dy but with overall smaller anisotropy. This field dependence indicates that dipolar physics is at least partially responsible for the anisotropic expansion dynamics, along with the isotope

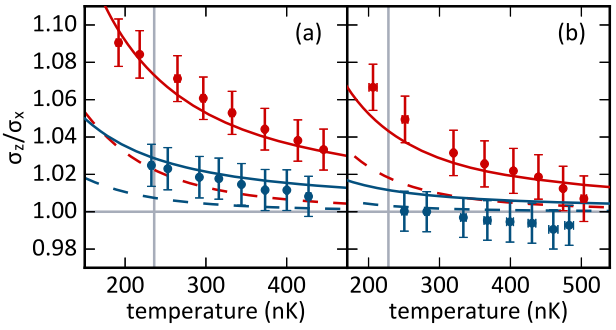

FIG. 1. Measured gas AR after 16 ms of TOF for ^{162}Dy in (a) and ^{164}Dy in (b). In both (a) and (b), red is for magnetic field along $\hat{z}$ and blue is for $\hat{y}$. Points are data with 1σ total error: statistical plus 1% systematic [26]. Solid red and blue curves are calculated using the full theory with the best-fit scattering lengths. Dashed curves are calculated for only the MF effect with the best-fit scattering lengths found using the full theory. Horizontal solid gray line marks unity AR and vertical gray line marks T_c.

dependence due to different scattering lengths [24], as we now explain.

Our starting point is the known phase-space distribution function of a classical noninteracting gas during expansion $f(\mathbf{r}, \mathbf{p}, t) = f_x(x, p_x, t) f_y(y, p_y, t) f_z(z, p_z, t)$, where $f_i(r_i, p_i, t) \propto \exp[-p_i^2/2mk_BT - m\omega_i^2(r_i - p_i t/m)^2/2k_BT]$. The spatial size along direction i evolves according to $\sigma_i(t) = \sqrt{k_BT/m\omega_i^2}\sqrt{1 + \omega_i^2 t^2}$, and in the limit $\omega_i t \gg 1$, we have $\sigma_i(t) \to \sqrt{k_BT/m}t$ leading to the isotropic shape in the long-time limit and reflecting the isotropic momentum distribution in the trap. Even in the presence of interactions, the rapidly decreasing density means that the expansion becomes ballistic, and therefore $\sqrt{\langle p_z^2\rangle/\langle p_x^2\rangle}$ determines σ_z/σ_x after a long TOF. We estimate the finite-t correction to σ_z/σ_x from the noninteracting case; it scales as $1/t^2$, and for our parameters it does not exceed 0.5%. Nevertheless, we take this effect into account.

The strategy for calculating $\langle p_i^2\rangle$ relies on a perturbative treatment. We write $\langle p_i^2\rangle = mk_BT + \Delta\langle p_i^2\rangle$, where mk_BT comes from the zeroth-order distribution function $f(\mathbf{r}, \mathbf{p}, t)$ and $\Delta\langle p_i^2\rangle$ takes into account interaction and statistical effects. The mean-field (MF) contribution to the kinetic energy $\Delta\langle p_i^2\rangle_{\mathrm{MF}}/2m$ equals work done by the ith component of the gradient of the MF interaction averaged over $f(\mathbf{r}, \mathbf{p}, t)$. This MF part contains the contact term, proportional to the scattering length a, and the dipole-dipole term, proportional to the dipole length $a_d = \mu_0\mu^2 m/8\pi\hbar^2$ [29], where μ_0 is the vacuum permeability. We find

$$\Delta\langle p_i^2\rangle_{\mathrm{MF}} = \frac{2N\hbar^2\bar{\omega}^3 m^{3/2}}{(k_BT)^{3/2}}\{a_d[H_d^{(i)} + F_d^{(i)}] + a[H^{(i)} + F^{(i)}]\}, \quad (1)$$

where $\bar{\omega} = (\omega_x\omega_y\omega_z)^{1/3}$ and the dimensionless constants H, H_d, F, and F_d, given explicitly in Ref. [26], are functions of the trap aspect ratios. These letters stand for the Hartree and Fock contributions, respectively. In addition, the dipole parts H_d and F_d depend on the field orientation [26]. Anisotropies due to the MF terms only are shown as dashed lines in Fig. 1. While the MF interaction is significant, it is not sufficient to match the level of anisotropy observed in our system.

We find that a more important contribution to the AR, independent of the MF term at leading order, is the thermalization during the TOF in which the kinetic energy is transferred from $\langle p_i^2\rangle/2m$ to $\langle p_j^2\rangle/2m$ by two-body collisions. In order to understand this phenomenon, we first point to the kinematic effect which occurs in the noninteracting gas and which can be seen from $f(\mathbf{r}, \mathbf{p}, t)$: during expansion the thermal motion of particles is transferred to the directed motion characterized by the finite average velocity with components $\langle v_i\rangle = r_i\omega_i^2 t/(1 + \omega_i^2 t^2)$. Important for us is that in the reference frame where the gas is locally stationary, its momentum distribution is equivalent to that of a thermal

gas with anisotropic temperature $T/(1+\omega_i^2 t^2)$ [26]. Collisions try to establish thermal equilibrium by transferring kinetic energy more frequently, on average, from "hotter" directions (smaller ω_i) to "colder" ones (larger ω_i). We call this effect hydrodynamic (HD), although the collision rate is too low to continuously maintain thermal equilibrium during expansion. The corresponding contribution to $\Delta\langle p_i^2\rangle$ is linear in the scattering cross section, i.e., quadratic in a and a_d,

$$\Delta\langle p_i^2\rangle_{\mathrm{HD}} = 2Nm^2 a_d^2 \bar{\omega}^2 \left\{ \left[A_0^{(i)} + A_1^{(i)} \left(\frac{a}{a_d}\right) + A_2^{(i)} \left(\frac{a}{a_d}\right)^2 \right] + N \left(\frac{\hbar\bar{\omega}}{k_{\mathrm{B}}T}\right)^3 \left[B_0^{(i)} + B_1^{(i)} \left(\frac{a}{a_d}\right) + B_2^{(i)} \left(\frac{a}{a_d}\right)^2 \right] \right\}, \tag{2}$$

where the dimensionless constants A and B are functions of the trap aspect ratios [26]. The first line in the right-hand side of Eq. (2) describes the two-body collisional effects using the differential cross sections obtained in the first-order Born approximation [26,30]. Previous work on inelastic dipolar collisions has shown the first-order Born approximation to be valid in strongly dipolar systems like dysprosium [31].

The last line in Eq. (2) accounts for the quantum effects on two-body collisions, where the probability of a scattering event is Bose enhanced according to the local phase-space density. This effect should be distinguished from the deviation of the *in situ* Bose-Einstein momentum distribution from the Maxwell-Boltzmann one. To first order in the degeneracy parameter, the *in situ* Bose-Einstein deviation is $\Delta\langle p_i^2\rangle_{\mathrm{BE}} = mk_{\mathrm{B}}T(N/16)(\hbar\bar{\omega}/k_{\mathrm{B}}T)^3$. It does not introduce any anisotropy to the gas AR, but it is important for the accurate determination of the temperature, even in the noninteracting gas. Adding this correction to the ones given by Eqs. (1) and (2) results in the *corrected* thermometry which infers $T = T_i$ from the expansion dynamics along direction i.

Among the four mechanisms labeled by letters H and F in Eq. (1) and A and B in Eq. (2), we find that the Hartree MF interaction (H) and the two-body collision effects (A) are the dominant sources of gas anisotropy: For the ^{162}Dy data point at 200 nK with field along $\hat{z}$ in Fig. 1(a), they contribute 3.0% and 5.6%, respectively, out of the total 9% anisotropy. These numbers are calculated for the aspect ratios $\omega_x:\omega_y:\omega_z = 107:49:266$ via Eqs. (28)–(37) of Ref. [26] (see Table I therein). We have also estimated the effective-range correction to the scattering cross sections by calculating the second-order Born correction to the interaction matrix element at finite collision energy. It is proportional to $a_d^2 k$, where $k \propto \sqrt{T}$ is the collision momentum. We find that the corresponding contribution to the AR is negligible for our parameters.

The MF interaction and the collisional effects cause the gas to expand faster in $\hat{z}$ but slower in $\hat{x}$ and $\hat{y}$ for our system's trap parameters. A direct application of the usual Bose-corrected TOF thermometry (neglecting interactions) in this case would yield conflicting apparent temperatures along each dimension. Indeed, this is shown by theoretical curves in Fig. 2(a). At 200 nK, the discrepancy $\Delta T = T_z - T_x$ between the two dimensions in the imaging plane is about 50 nK, corresponding to 25% of its temperature. A mistaken application of this theory leads to an inaccurate determination of temperature and other temperature-related properties such as gas size, trap density, etc., highlighting the need for the corrections in Eqs. (1) and (2).

The fact that a gas in thermal equilibrium has a single well-defined temperature allows us to determine the decaheptuplet s-partial-wave scattering length a of ^{162}Dy and ^{164}Dy using our theory. With the correct a value, our theory should both minimize ΔT and predict the measured AR at various temperatures. To determine a, we vary a in Eqs. (1) and (2) and find the best-fit scattering length that simultaneously matches the AR data measured at the two different field orientations. In this fitting procedure, we assign the average of T_x and T_z to be the gas temperature. The details of this analysis are described in [26]. The fitted scattering length is $a_{162} = 154(22)a_0$ for ^{162}Dy and $a_{164} = 96(22)a_0$ for ^{164}Dy, where a_0 is the Bohr radius. This new measurement for ^{164}Dy is consistent with our previously reported value, $92(8)a_0$, measured in cross-dimensional relaxation experiments [24]. It also agrees with the measurement reported in Ref. [17] using Feshbach spectroscopy. The new best-fit a for ^{162}Dy is larger than, though not inconsistent with, our previous measurement $122(10)a_0$, and we provide a more detailed discussion of this discrepancy in the Supplemental Material [26].

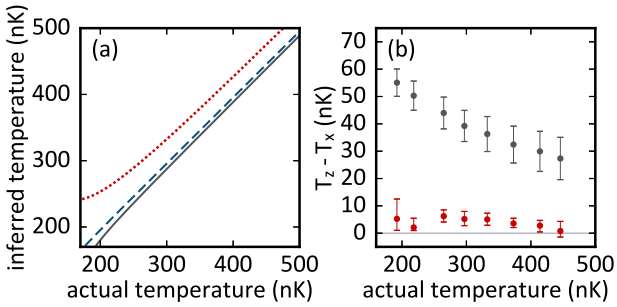

FIG. 2. (a) Illustration of Bose-corrected TOF thermometry to a dipolar thermal Bose gas, showing that the theory fails to yield the same temperature along the $\hat{x}$, $\hat{y}$, and $\hat{z}$ directions. Field along $\hat{z}$. Theory curves are T_x (blue, dashed), T_y (gray, solid), and T_z (red, dotted). (b) Observed difference between T_x and T_z, the two dimensions in the imaging plane. The discrepancy is large if only the Bose-corrected TOF thermometry is applied directly (gray points), but can be reduced to close to zero (gray line) using the additional corrections provided in Eqs. (1) and (2) (red points). Theoretical curves in (a) and data in (b) are presented for the experimental parameters used in the ^{162}Dy measurement of Fig. 1(a) with the magnetic field along $\hat{z}$: $N = 1.4(1)\times 10^5$ and $[\omega_x,\omega_y,\omega_z] = 2\pi\times[107(1),49(5),266(1)]$ Hz.

To illustrate that our theory greatly improves the accuracy of thermometry for a thermal dipolar Bose gas, we show in Fig. 2(b) ΔT before and after applying our theory to the ^{162}Dy measurement. The ΔT measured in Fig. 2(b) increases at lower temperatures and is similar to the theoretical predictions for Bose-corrected TOF thermometry in Fig. 2(a). Applying our corrections with the best-fit scattering length leads to almost an order of magnitude reduction in ΔT. This allows us to determine the temperature of a thermal dipolar Bose gas with far less uncertainty. The temperatures assigned to the data in Fig. 1 are the average of the corrected T_x and T_z; error bars represent the discrepancy.

The dependence of gas AR on the scattering length a provides an experimental probe for investigating the variation of a near Feshbach resonances. For magnetic Feshbach resonances, a varies with the magnetic field B according to $a(B) = a_{bg}[1 - \Delta B/(B - B_0)]$, where a_{bg} is the background scattering length, B_0 is the resonance center, and ΔB is the resonance width [19]. We demonstrate the measurement of a near a Feshbach resonance at 5.1 G for ^{162}Dy, shown in Fig. 3(a), by analyzing the gas AR in TOF.

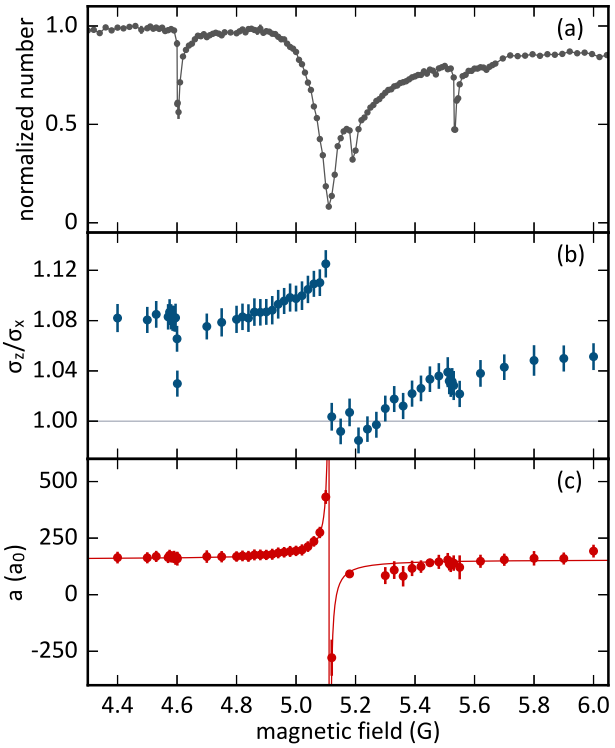

FIG. 3. (a) High resolution atom-loss spectrum for ^{162}Dy showing a resonance at 5.1 G and three nearby narrower resonances. Line is to guide the eye. (b) Measured gas AR as a function of magnetic field. Horizontal line marks unity AR. (c) Scattering lengths corresponding to the data in (b). We are unable to extract a scattering length for four points near the 5.2 G small resonance with AR below unity; see text for details. All error bars represent 1σ uncertainty.

Our technique is more convenient than cross-dimensional relaxation for measuring scattering length because it requires only a single experimental measurement to determine a at a given field. Cross-dimensional relaxation, by contrast, requires multiple measurements to extract a thermalization time as well as extensive numerical simulations when a strong dipolar interaction is present [32,33].

To measure the gas AR near the resonance, we prepare $2.7(1) \times 10^5$ atoms at 280 nK in a trap with $[\omega_x, \omega_y, \omega_z] = 2\pi \times [89(1), 44(5), 219(1)]$ Hz. The magnetic field is first set at 1.580(5) G, which is the value used for evaporative cooling. We then shift the field to the desired value using a 10-ms linear ramp. Throughout this procedure, the field is kept along the axis of tight confinement, $\hat{z}$, to achieve the largest anisotropy in AR. After the field ramp, we hold the atoms for 50 ms before releasing for TOF imaging.

The measured gas ARs are shown in Fig. 3(b). As the field approaches the 5.1-G resonance from the lower side, we observe increasingly larger AR, as is expected for larger a. We use our theory to convert the AR values to scattering length, accounting for variations in atom number. The results are shown in Fig. 3(c). The AR that follows from Eqs. (1) and (2) is a quadratic function of a given by $\sigma_z/\sigma_x \approx 1.01 + [2.3 \times 10^{-4} + 1.6 \times 10^{-6}(a/a_0)](a/a_0)$ for the ω's, N, and T mentioned above. A minimum value therefore occurs at $a \approx -72a_0$ with $\sigma_z/\sigma_x \approx 1$. With our 1% systematic error, we therefore have a *blind spot* in scattering length in the region $-139a_0 \lesssim a \lesssim -4a_0$ about $a \approx -72a_0$. It is within this range wherein the four data points near 5.2 G that have ARs below (but within $\sim 1.5\sigma$ of) the theoretical minimum value presumably lie, and we are unable to determine a scattering length for them [35]. In principle, this blind spot could be shifted to a different region of a by adjusting trap aspect ratios.

The scattering lengths shown in Fig. 3(c) fit well to the functional form $a(B)$. The fitted resonance width is $\Delta B = 24(2)$ mG, and the fitted background scattering length is $a_{bg} = 157(4)a_0$. This a_{bg} value is consistent with the best-fit a_{162} obtained from analysis of the data shown in Fig. 1(a), which are taken at a different field and trap frequency with about half the atom number. Note that we do not observe a measurable change in a at the other two small resonances near 4.6 G and 5.6 G.

In conclusion, we observe and develop a theoretical understanding of the anisotropic expansion of *thermal* dipolar Bose gases of ^{162}Dy and ^{164}Dy. The experiment lies in a very favorable regime as far as experiment-theory comparison is concerned; the AR anisotropy is large enough to be measured though small enough for a well-controlled perturbative theory to apply. As a consequence, we are able to apply this theory for TOF thermometry in this novel regime as well as measure the scattering length of the gas near a Feshbach resonance with ease. This simple method for measuring scattering lengths may contribute to

the development of a comprehensive theoretical understanding of how collisions are affected within the dense and ultradense Feshbach spectra of these collisionally complex lanthanide atoms [16–18,36]. Looking beyond the study of hydrodynamics in magnetic Bose gases, a similar thermometry theory may aid the study of polar molecules near quantum degeneracy.

We acknowledge experimental assistance from Wil Kao, helpful discussions with Matthew Davis, and support from AFOSR, NSF, and the IFRAF Institute. The research leading to these results received funding from the European Research Council (FP7/2007–2013 Grant Agreement No. 341197), and the European Union's Horizon 2020 research and innovation program under Grant Agreement No. 658311. J. D. and Y. T. acknowledge partial support from a Karel Urbanek Postdoctoral Fellowship and a Stanford Graduate Fellowship, respectively.

[1] M. H. Anderson, J. R. Ensher, M. R. Matthews, C. E. Wieman, and E. A. Cornell, Observation of Bose-Einstein condensation in a dilute atomic vapor, Science **269**, 198 (1995).

[2] K. B. Davis, M. O. Mewes, M. R. Andrews, N. J. van Druten, D. S. Durfee, D. M. Kurn, and W. Ketterle, Bose-Einstein Condensation in a Gas of Sodium Atoms, Phys. Rev. Lett. **75**, 3969 (1995).

[3] I. Shvarchuck, Ch. Buggle, D. S. Petrov, M. Kemmann, W. von Klitzing, G. V. Shlyapnikov, and J. T. M. Walraven, Hydrodynamic behavior in expanding thermal clouds of ^{87}Rb, Phys. Rev. A **68**, 063603 (2003).

[4] A. Trenkwalder, C. Kohstall, M. Zaccanti, D. Naik, A. I. Sidorov, F. Schreck, and R. Grimm, Hydrodynamic Expansion of a Strongly Interacting Fermi-Fermi Mixture, Phys. Rev. Lett. **106**, 115304 (2011).

[5] P. Pedri, D. Guéry-Odelin, and S. Stringari, Dynamics of a classical gas including dissipative and mean-field effects, Phys. Rev. A **68**, 043608 (2003).

[6] T. Lahaye, C. Menotti, L. Santos, M. Lewenstein, and T. Pfau, The physics of dipolar bosonic quantum gases, Rep. Prog. Phys. **72**, 126401 (2009).

[7] M. Lu, N. Q. Burdick, S.-H. Youn, and B. L. Lev, Strongly Dipolar Bose-Einstein Condensate of Dysprosium, Phys. Rev. Lett. **107**, 190401 (2011).

[8] K. Aikawa, S. Baier, A. Frisch, M. Mark, C. Ravensbergen, and F. Ferlaino, Observation of Fermi surface deformation in a dipolar quantum gas, Science **345**, 1484 (2014).

[9] Anisotropic expansion of quantum degenerate dipolar Bose and Fermi gases have been explored in Refs. [6–8].

[10] K. Baumann, N. Q. Burdick, M. Lu, and B. L. Lev, Observation of low-field Fano-Feshbach resonances in ultracold gases of dysprosium, Phys. Rev. A **89**, 020701(R) (2014).

[11] L. P. Pitaevskii and E. M. Lifshitz, *Physical Kinetics*, Landau and Lifshitz, Course of Theoretical Physics, Vol. 10 (Elsevier Science, New York, 2012).

[12] W. D. McComb, *The Physics of Fluid Turbulence*, Oxford Engineering Science Series (Clarendon Press, New York, 1992); Uriel Frisch, *Turbulence: The Legacy of A. N. Kolmogorov* (Cambridge University Press, Cambridge, 1995); M. Lesieur, *Turbulence in Fluids, Fluid Mechanics and Its Applications* (Springer, The Netherlands, 2008).

[13] J. P. McTague, Magnetoviscosity of magnetic colloids, J. Chem. Phys. **51**, 133 (1969); W. F. Hall and S. N. Busenberg, Viscosity of magnetic suspensions, J. Chem. Phys. **51**, 137 (1969); M. I. Shliomis, Effective viscosity of magnetic suspensions, Sov. Phys. JETP **34**, 1291 (1972); M. A. Martsenyuk, Yu. L. Raikher, and M. I. Shliomis, On the kinetics of magnetization of suspensions of ferromagnetic particles, Sov. Phys. JETP **38**, 413 (1974).

[14] L Skrbek, Quantum turbulence, J. Phys. Conf. Ser. **318**, 012004 (2011); M. T. Reeves, B. P. Anderson, and A. S. Bradley, Classical and quantum regimes of two-dimensional turbulence in trapped Bose-Einstein condensates, Phys. Rev. A **86**, 053621 (2012); M. Tsubota, Turbulence in quantum fluids, J. Stat. Mech. Theor. Exp. **2014**, P02013 (2014).

[15] K. Aikawa, A. Frisch, M. Mark, S. Baier, A. Rietzler, R. Grimm, and F. Ferlaino, Bose-Einstein Condensation of Erbium, Phys. Rev. Lett. **108**, 210401 (2012).

[16] A. Frisch, M. Mark, K. Aikawa, F. Ferlaino, J. L. Bohn, C. Makrides, A. Petrov, and S. Kotochigova, Quantum chaos in ultracold collisions of gas-phase erbium atoms, Nature (London) **507**, 475 (2014).

[17] T. Maier, I. Ferrier-Barbut, H. Kadau, M. Schmitt, M. Wenzel, C. Wink, T. Pfau, K. Jachymski, and P. S. Julienne, Broad universal feshbach resonances in the chaotic spectrum of dysprosium atoms, Phys. Rev. A **92**, 060702(R) (2015).

[18] T. Maier*et al.*, Emergence of Chaotic Scattering in Ultracold Er and Dy, Phys. Rev. X **5**, 041029 (2015).

[19] C. Chin, R. Grimm, P. Julienne, and E. Tiesinga, Feshbach resonances in ultracold gases, Rev. Mod. Phys. **82**, 1225 (2010).

[20] A. Griesmaier, J. Stuhler, T. Koch, M. Fattori, T. Pfau, and S. Giovanazzi, Comparing Contact and Dipolar Interactions in a Bose-Einstein Condensate, Phys. Rev. Lett. **97**, 250402 (2006).

[21] Y. Tang, N. Q. Burdick, K. Baumann, and B. L. Lev, Bose-Einstein condensation of ^{162}Dy and ^{160}Dy, New J. Phys. **17**, 045006 (2015).

[22] Uncertainties are given as standard errors.

[23] σ is the standard deviation of the Gaussian profile.

[24] Y. Tang, A. Sykes, N. Q. Burdick, J. L. Bohn, and B. L. Lev, *s*-wave scattering lengths of the strongly dipolar bosons ^{162}Dy and ^{164}Dy, Phys. Rev. A **92**, 022703 (2015); **93**, 059905(E) (2016).

[25] T. Koch, T. Lahaye, J. Metz, B. Frohlich, A. Griesmaier, and T. Pfau, Stabilization of a purely dipolar quantum gas against collapse, Nat. Phys. **4**, 218 (2008).

[26] See Supplemental Material at http://link.aps.org/supplemental/10.1103/PhysRevLett.117.155301, which includes Refs. [24,27,28], for information on experimental details, theory, data analysis, and scattering lengths.

[27] I. Hughes and T. Hase, *Measurements and Their Uncertainties: A Practical Guide to Modern Error Analysis* (Oxford University Press, New York, 2010).

[28] R. C. Paule and J. Mandel, Consensus values and weighting factors, J. Res. Natl. Bur. Stand. **87**, 377 (1982).

[29] J. L. Bohn, M. Cavagnero, and C. Ticknor, Quasi-universal dipolar scattering in cold and ultracold gases, New J. Phys. **11**, 055039 (2009).

[30] J. L. Bohn and D. S. Jin, Differential scattering and rethermalization in ultracold dipolar gases, Phys. Rev. A **89**, 022702 (2014).

[31] N. Q. Burdick, K. Baumann, Y. Tang, M. Lu, and B. L. Lev, Fermionic Suppression of Dipolar Relaxation, Phys. Rev. Lett. **114**, 023201 (2015).

[32] A. G. Sykes and J. L. Bohn, Nonequilibrium dynamics of an ultracold dipolar gas, Phys. Rev. A **91**, 013625 (2015).

[33] An alternative method is to measure the energy gap in the Mott insulating phase at unit filling factor [34].

[34] M. Mark (private communication).

[35] Atom loss is significant near the resonance center, making the blind spot region in scattering length even larger.

[36] Nathaniel Q Burdick, Yijun Tang, and Benjamin L Lev, Long-Lived Spin-Orbit-Coupled Degenerate Dipolar Fermi Gas, Phys. Rev. X **6**, 031022 (2016).